Int. J. Heat Mass Transfer. Vol. 6, pp. 537–557. Pergamon Press 1963. Printed in Great Britain.

HEAT TRANSFER IN ANNULAR PASSAGES—HYDRODYNAMICALLY DEVELOPED TURBULENT FLOW WITH ARBITRARILY PRESCRIBED HEAT FLUX

W. M. KAYS† and E. Y. LEUNG‡

(*Received* 15 *December* 1962)

Abstract—The problem of turbulent flow heat transfer in a concentric circular tube annulus with fully developed velocity profile and constant heat rate per unit of length is considered. Experimentally obtained solutions are presented for the thermal entry length for a fluid with $Pr = 0{\cdot}7$. Asymptotic solutions (fully developed velocity and temperature profiles) are developed for a wide range of radius ratio, Reynolds number, and Prandtl number. The solutions are based on empirical velocity and eddy diffusivity profiles, and the validity of the solutions is demonstrated experimentally for $Pr = 0{\cdot}7$. A superposition method is demonstrated for solving the problem of asymmetric heating from the two surfaces of an annulus, and experimental data on asymmetric heating are presented which are in excellent agreement with the analysis. This paper is the third in a series (1, 2) culminating a four year study of heat transfer in annular passages.

NOMENCLATURE

- c_p, specific heat at constant pressure;
- D_h, hydraulic diameter, $2(r_o - r_i)$;
- h_j, unit convection conductance at surface j;
- k, thermal conductivity;
- n, co-ordinate normal to a tube surface;
- q_j'', heat flux at surface j;
- r, radial co-ordinate of annulus geometry, measured from axis;
- s, radius of maximum axial velocity;
- t, temperature;
- u, local axial velocity;
- V, mean velocity;
- x, axial co-ordinate of annulus geometry;
- y_j, radial co-ordinate of annulus geometry measured from surface j.

Greek symbols

- α, thermal molecular diffusivity;
- ϵ_H, thermal eddy diffusivity;
- ϵ_M, momentum eddy diffusivity;
- η_j, non-dimensional radial co-ordinate, referred to surface j, $(s - r)/(s - r_j)$;
- θ, non-dimensional temperature, defined by equation (2);
- ν, kinematic viscosity;
- ξ, dummy axial variable, dimensionally similar to x;
- ρ, density;
- τ, total apparent shear stress;
- Φ_j, non-dimensional heat flux at surface j, defined by equation (2).

Non-dimensional groupings

- Nu_j, Nusselt number at surface j, $h_j D_h/k$;
- Pr, Prandtl number, $\rho\nu c_p/k$;
- Re, Reynolds number, $D_h V/\nu$;
- r^*, annulus radius ratio, r_i/r_o;
- τ^*, surface shear stress ratio;
- $\bar{s}$, s/r_o;
- s^*, $(\bar{s} - r^*)/(1 - \bar{s})$;
- u_j^+, non-dimensional axial velocity referred to shear velocity at surface j, $u/\sqrt{(\tau_j/\rho)}$;
- y_j^+, non-dimensional distance in radial direction from surface j, $y_j\sqrt{(\tau_j/\rho)}/\nu$;
- η_j^+, modified radial co-ordinate measured from surface j, $1{\cdot}5\, y_j^+ (1 + \eta_j)/(1 + 2\eta_j^2)$.

† Professor of Mechanical Engineering, Stanford University, Stanford, California.

‡ Research Assistant, Mechanical Engineering, Stanford University, Stanford, California.

Subscripts

- e, entrance of tube;
- j, either the inner or outer surface of the annulus flow passage;
- i, inner surface;
- o, outer surface;
- ii, inner surface conditions, when inner surface alone is heated;
- oo, outer surface conditions, when outer surface alone is heated;
- io, inner surface conditions when outer surface alone is heated;
- oi, outer surface conditions when inner surface alone is heated;
- mi, mixed mean conditions when inner surface alone is heated;
- mo, mixed mean conditions when outer surface alone is heated.

INTRODUCTION AND OBJECTIVES

THIS PAPER has been prepared as part of a series [1, 2] on steady heat convection in a circular tube annular passage. In the first paper [1], it is shown how the general problem of arbitrarily specified heat flux and/or surface temperatures on the two surfaces of an annulus can be solved by superposition employing one or more of four fundamental solutions to the energy equation. The second paper [2] contains a complete development of the four fundamental solutions for hydrodynamically developed *laminar* flow in a concentric annulus. The present paper is concerned with the same problem, but for *turbulent* flow.

The turbulent flow problem is two orders of magnitude more complex than its laminar flow counterpart because Reynolds number and Prandtl number become parameters, and it is beset with further difficulties because of our incomplete knowledge of the details of the turbulent heat transport mechanism. Thus, this paper will be less complete than the previous one, and, in fact, of the four fundamental solutions, only the Fundamental Solutions of the Second Kind are considered, and these only in incomplete form. Nevertheless, sufficient data, both analytic and experimental, are presented to solve a large variety of annulus heat convection problems in which heat flux on the surfaces is specified.

For four annulus radius ratios, 0·192, 0·255, 0·376, and 0·500, the Fundamental Solutions of the Second Kind are developed completely for air ($Pr = 0{\cdot}7$) entirely from experimental data. An asymptotic solution is then developed analytically (velocity and temperature profiles fully developed) for Prandtl number from 0 to 10^3, Reynolds number from 10^4 to 10^6, and radius ratio from 0·1 to 1·0. This solution is shown to be in excellent agreement with experiment for $Pr = 0{\cdot}7$. Finally, experimental data are presented for several cases of asymmetric heating, and these are shown to be in excellent agreement with predictions from the fundamental solutions.

ENERGY DIFFERENTIAL EQUATION AND THE FUNDAMENTAL SOLUTIONS OF THE SECOND KIND

Under conditions of steady hydrodynamically fully developed turbulent flow with constant fluid properties, negligible axial conduction, and axially symmetric heating, the energy differential equation may be written as follows if it is assumed that an eddy diffusivity can be rationally defined:

$$\frac{\partial}{\partial r}\left[r(\epsilon_H + \alpha)\frac{\partial t}{\partial r}\right] = ru(r)\frac{\partial t}{\partial x}. \qquad (1)\dagger$$

At the axial distance $x = 0$ let the fluid and both of the wall surfaces be at a uniform temperature t_e. At this point, let the heat flux on either the core wall or the outer wall, j, be increased stepwise to a constant q_j'' while the opposite wall is insulated. Let a non-dimensional fluid temperature and surface heat flux be defined as,

$$\theta^{(2)} = \frac{t - t_e}{q_j'' D_h/k} \qquad \Phi_j^{(2)} = D_h\left(\frac{\partial\theta}{\partial n}\right)_j. \qquad (2)$$

Then the boundary conditions become,

$$\Phi_j^{(2)} = \begin{cases} 1, \text{ on the heated wall} \\ 0, \text{ on the opposite wall} \end{cases}, x > 0,$$

$$\theta^{(2)} = 0, x \leqslant 0. \qquad (3)$$

The nomenclature employed here is identical with that of reference [1]. Since we deal here with

† See [1], equation (1), for a more general form of (1).

solutions of the Second Kind, the superscript (2) will henceforth be omitted.

The problem then reduces to

(1) seeking the fundamental solutions, $\theta_{ii}(x)$, $\theta_{oi}(x)$, and $\theta_{mi}(x)$, for the boundary conditions, $\Phi_{ii} = 1$, and $\Phi_{oi} = 0$,

(2) seeking the fundamental solutions, $\theta_{oo}(x)$, $\theta_{io}(x)$, and $\theta_{mo}(x)$, for the boundary conditions, $\Phi_{oo} = 1$, and $\Phi_{io} = 0$.

With these fundamental solutions the inner and outer surface temperatures and the mixed mean fluid temperature can be calculated for any arbitrarily specified axial flux distribution on either surface by taking advantage of the linearity of (1) and using superposition. For hydrodynamically fully developed axi-symmetric flow the fundamental solutions are only functions of the distance from the discontinuity in the boundary condition. Then from the general solution of the Second Kind, Table 1, reference [1], it follows that,

$$t_i(x) = \frac{D_h}{k}\int_{\xi=0}^{\xi=x} \theta_{ii}(x-\xi)\,\mathrm{d}q_i''(\xi) + \frac{D_h}{k}\int_{\xi=0}^{\xi=x} \theta_{io}(x-\xi)\,\mathrm{d}q_o''(\xi) + t_e. \quad (4)$$

$$t_o(x) = \frac{D_h}{k}\int_{\xi=0}^{\xi=x} \theta_{oi}(x-\xi)\,\mathrm{d}q_i''(\xi) + \frac{D_h}{k}\int_{\xi=0}^{\xi=x} \theta_{oo}(x-\xi)\,\mathrm{d}q_o''(\xi) + t_e. \quad (5)$$

$$t_m(x) = \frac{D_h}{k}\int_{\xi=0}^{\xi=x} \theta_{mi}(x-\xi)\,\mathrm{d}q_i''(\xi) + \frac{D_h}{k}\int_{\xi=0}^{\xi=x} \theta_{mo}(x-\xi)\,\mathrm{d}q_o''(\xi) + t_e. \quad (6)$$

For the more restricted case of a *constant* heat flux, q_i'', on the inner wall and a *constant* heat flux, q_o'', on the outer wall, (4), (5), and (6) reduce to the following:

$$t_i(x) = \frac{D_h}{k}\,[\theta_{ii}(x)\,q_i'' + \theta_{io}(x)\,q_o''] + t_e \quad (7)$$

$$t_o(x) = \frac{D_h}{k}\,[\theta_{oi}(x)\,q_i'' + \theta_{oo}(x)\,q_o''] + t_e \quad (8)$$

$$t_m(x) = \frac{D_h}{k}\,[\theta_{mi}(x)\,q_i'' + \theta_{mo}(x)\,q_o''] + t_e. \quad (9)$$

By subtraction the entrance temperature can be eliminated and the temperature differences between the fluid mixed mean and the two surfaces can be calculated.

$$t_i(x) - t_m(x) = \frac{D_h}{k}\,\{[\theta_{ii}(x) - \theta_{mi}(x)]\,q_i'' + [\theta_{io}(x) - \theta_{mo}(x)]\,q_o''\}. \quad (10)$$

$$t_o(x) - t_m(x) = \frac{D_h}{k}\,\{[\theta_{oi}(x) - \theta_{mi}(x)]\,q_i'' + [\theta_{oo}(x) - \theta_{mo}(x)]\,q_o''\}. \quad (11)$$

For the case where $q_o'' = 0$, equation (10) becomes,

$$t_i(x) - t_m(x) = \frac{D_h}{k}\,[\theta_{ii}(x) - \theta_{mi}(x)]\,q_i''.$$

For convenience a Nusselt number can be defined for the inner surface:

$$Nu_i(x) = \frac{D_h}{k}\,\frac{q_i''}{[t_i(x) - t_m(x)]}. \quad (12)$$

Then if the inner surface alone is heated, Nu_i becomes Nu_{ii} according to the subscript convention, and it follows that,

$$Nu_{ii}(x) = \frac{1}{\theta_{ii}(x) - \theta_{mi}(x)} \quad (13)$$

similarly,

$$Nu_{oo}(x) = \frac{1}{\theta_{oo}(x) - \theta_{mo}(x)}. \quad (14)$$

For the more general case of both surfaces heated (but at independently specified heat fluxes) the Nusselt number defined by equation (12) is still useful and may be evaluated by substituting equation (10) into (12). Making use of (13) and defining influence coefficients, θ_i^* and θ_o^*, the following simple expressions for the Nusselt numbers on the two surfaces for asymmetric heating are obtained:

$$Nu_i(x) = \frac{Nu_{ii}(x)}{1 - \theta_i^*(x)\cdot q_o''/q_i''} \quad (15)$$

$$Nu_o(x) = \frac{Nu_{oo}(x)}{1 - \theta_o^*(x)\cdot q_i''/q_o''} \quad (16)$$

where,

$$\theta_i^*(x) = \frac{\theta_{mo}(x) - \theta_{io}(x)}{\theta_{ii}(x) - \theta_{mi}(x)} \qquad (17)$$

$$\theta_o^*(x) = \frac{\theta_{mi}(x) - \theta_{oi}(x)}{\theta_{oo}(x) - \theta_{mo}(x)}. \qquad (18)$$

It should be emphasized that to solve problems where the heat flux on the two surfaces *varies axially* equations (4), (5), and (6) must be employed. If the heat flux on the two surfaces is *constant* (though different) equations (7)–(16) are all applicable in *both* the thermal entry region and the fully developed region far downstream. In the sections to follow, the various $\theta(x)$ are presented for a variety of radius ratios and Reynolds numbers but only for a fluid with $Pr = 0{\cdot}7$. Thus, it is only for $Pr = 0{\cdot}7$ that thermal entry length and axially varying heat flux problems can be solved with the data given herein. However, for the thermally fully developed region ($x \to \infty$) Nu_{ii}, Nu_{oo}, θ_i^*, and θ_o^* are presented for all Prandtl numbers from 0 to 1000. For most engineering applications, with the exception of the low Prandtl number liquid metal region, thermal entry length and axial heat flux variation effects are not particularly significant, whereas asymmetric heating effects (q_i''/q_o'') may be quite significant. Thus the solutions for thermally fully developed flow are by no means of restricted usefulness but rather form the more important part of this paper. For *laminar* flow, like low Prandtl number turbulent flow, the thermal entry region solutions are of extreme importance and are given completely in [2].

Note that q_i'' and q_o'' are defined as positive *into* the fluid. The solutions are equally applicable whether the heat flux ratio is positive or negative. It is quite possible to have a negative Nusselt number under asymmetric heating conditions, and this does not destroy either the validity or the usefulness of the Nusselt number.

EXPERIMENTAL APPARATUS

The experimental apparatus employed to establish the Fundamental Solutions of the Second Kind for $Pr = 0{\cdot}7$ is described in complete detail in [3], and somewhat less completely in [1].

DATA REDUCTION

To determine the fundamental solutions from the experimental measurements, equations (10) and (11) were used directly. Series of tests were run at various Reynolds numbers with the inner tube heated, and then the outer tube heated. The mean fluid temperature at each point along the tube was evaluated by integration of the heat flux up to that point and making an energy balance. Where the outer tube was heated the heat flux was first corrected by deducting the calibrated heat leak. In all of the tests there was some radiation between the surfaces, and the radiation rate was estimated assuming an emissivity for Inconel of 0·35. Because of the radiation, no tests were actually run with heat convection from one surface only, although the heat radiated across the passage and conducted into the air from the opposite side was small relative to that directly conducted to the air from the heated surface. A method was developed, involving some minor approximations, so that all four of the dimensionless temperature differences in (10) and (11) could be evaluated from the two sets of tests, even though the heating was slightly asymmetric.

All fluid properties were evaluated at local mixed mean temperature. To avoid difficulties with the influence of temperature dependent fluid properties the heat fluxes were adjusted so that local temperature differences were never more than about 50°F. Nevertheless, a correction taking into consideration this effect was made by assuming that the dimensionless temperature differences vary as the absolute temperature ratio, surface to mean fluid, to the 0·575 power, since this is the effect that may be deduced from the large temperature difference circular tube data of Humble *et al.* [4]. The correction is thus a maximum of about 5 per cent.

The heated length-to-hydraulic-diameter ratio of the tubes varied from 23 for the 0·192 radius ratio tube to 73 for the 0·500 radius ratio tube. Thus, for none of the tubes was it possible to measure directly the asymptotic temperature differences (or Nusselt numbers) since some remnant of the thermal entry length would still be in evidence even at these lengths. To determine the asymptotic solutions, an extrapolation was employed based on the reasonable assumption that the tube-length dependence of the solution may be approximated by the first term of the exact infinite series solution, which is a simple exponential. $\theta_{ii} - \theta_{mi}$ and $\theta_{oo} - \theta_{mo}$ were plotted as functions of x, a smooth curve was drawn through the data points, and then the last 5 per cent of the rise of the curve was employed as the basis for the extrapolation. The data along a half to three-quarters of the heated length of the tube was generally in this 5 per cent region, and the resulting extrapolation yielded an asymptotic solution that typically differed from the last data point by 0·5 to 4·0 per cent.

The temperature differences, $\theta_{mo} - \theta_{io}$ and $\theta_{mi} - \theta_{oi}$, are much more difficult to establish experimentally because they are very small relative to the other differences and are very sensitive to small experimental uncertainties. This is especially true of θ_{oi} where a small amount of heat leak has a large effect. By the same token, these differences are much less important in application of the results. In the data presented, these differences are based partially on the experimental measurements and partially on the asymptotic behavior predicted in the analytical section of this paper.

A complete analysis of the experimental uncertainty is presented in [3], and the conclusions only will be given here. The expected uncertainty in the dimensionless mean temperature differences (Nusselt number inverses) for the case of the inner tube alone heated is $\pm 3{\cdot}2$ per cent. For the outer tube alone heated, the estimated uncertainty is $\pm 2{\cdot}6$ per cent. The uncertainty in the Reynolds number determination is $\pm 2{\cdot}0$ per cent.

The best verification of the low uncertainty estimates lies in the excellent correlation between analysis and experiment obtained in the laminar flow work reported by Lundberg, McCuen and Reynolds [2] using the same apparatus and the same procedures. Virtually all of the sources of error are greatly magnified at the very low flow rates employed in the laminar flow experiments.

EXPERIMENTALLY DETERMINED FUNDAMENTAL SOLUTIONS OF THE SECOND KIND

The fundamental solutions deduced from the experimental measurements are presented in Figs. 1, 2, 3, and 4. Each figure covers one radius ratio and five different turbulent flow Reynolds numbers. All of the fundamental solutions of the

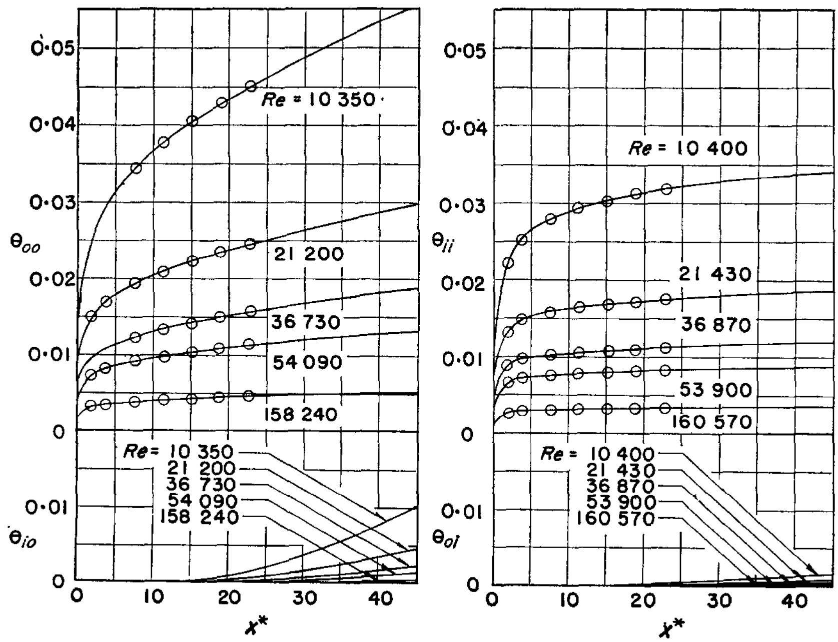

FIG. 1. Fundamental solutions of the second kind for $r^* = 0{\cdot}192$ and $Pr = 0{\cdot}70$.

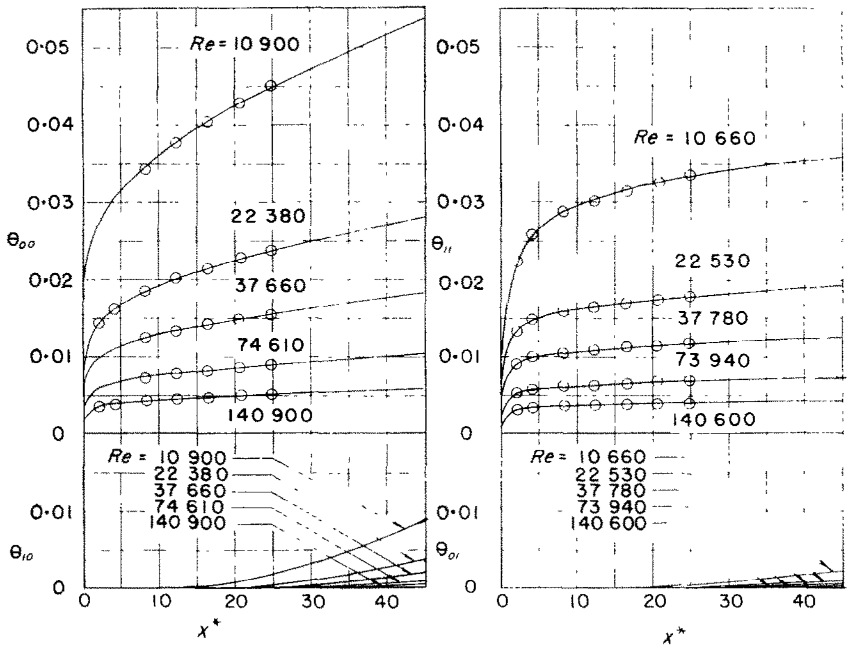

FIG. 2. Fundamental solutions of the second kind for $r^* = 0{\cdot}255$ and $Pr = 0{\cdot}70$.

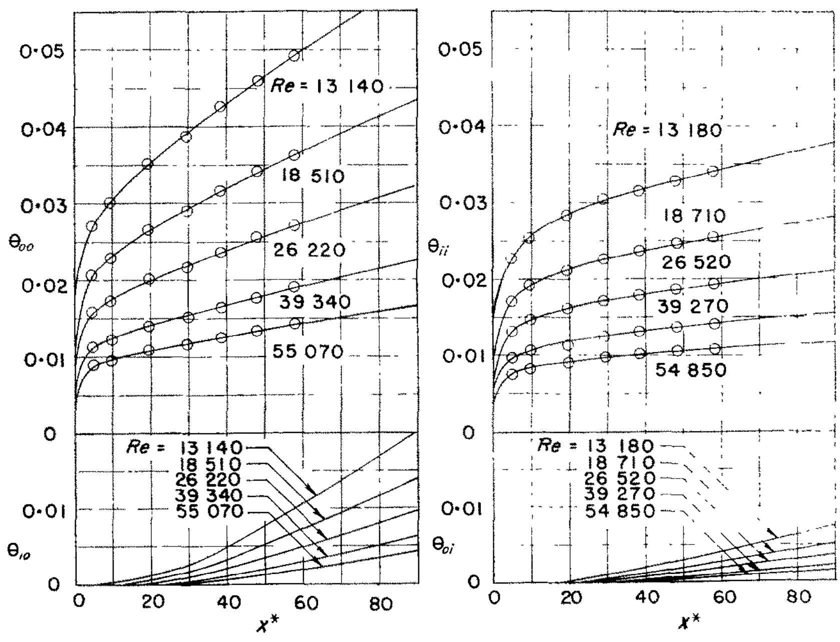

FIG. 3. Fundamental solutions of the second kind for $r^* = 0{\cdot}376$ and $Pr = 0{\cdot}70$.

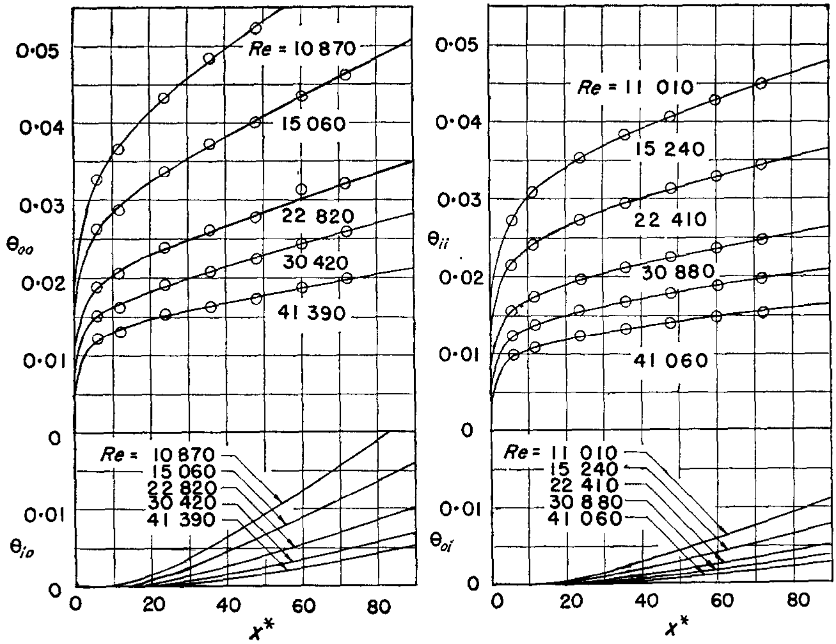

FIG. 4. Fundamental solutions of the second kind for $r^* = 0{\cdot}500$ and $Pr = 0{\cdot}70$.

second kind are plotted with the exception of θ_{mi} and θ_{mo}. These latter can be established by simple energy balances and expressed in algebraic form.

$$\theta_{mi} = \frac{4r^* (x/D_h)}{Re\,Pr\,(1 + r^*)} \tag{19}$$

$$\theta_{mo} = \frac{4\,(x/D_h)}{Re\,Pr\,(1 + r^*)}. \tag{20}$$

These solutions can now be used directly in equations (4), (5), and (6) for calculation of any arbitrary heat flux distribution on the two surfaces of the annulus, as well as in the more restricted equations (7)–(18).

The solutions are, of course, limited to a fluid with $Pr = 0{\cdot}7$ and are restricted to the particular radius ratios and Reynolds numbers of the tests. However, cross-plotting and interpolation could be employed to increase the generality of the results.

EXPERIMENTAL RESULTS FOR FULLY DEVELOPED CONSTANT HEAT RATE

In a previous section the method of extrapolation of the thermal entry length data to obtain the asymptotic solutions is described. These results have been reduced to Nusselt numbers and plotted in Figs. 5 to 10.

The results for the circular tube plotted in Fig. 5 were obtained to provide another check on the experimental apparatus, and alsc, of course, because the circular tube is one of the limiting cases of the annulus. For comparison purposes, the analytic solution of Sparrow, Hallman, and Siegel [5] is plotted, as well as the solution described in the next section of this paper, and the following empirical equation which has been used by the authors to correlate a large amount of experimental data for the constant heat rate asymptotic Nusselt number for fluids in the gas Prandtl number range.

$$Nu = 0{\cdot}022\,Pr^{0{\cdot}5}\,Re^{0{\cdot}8}. \tag{21}$$

The test results are seen to agree very well with both of the analytic solutions as well as with the empirical equation.

Figs. 6–9 show the asymptotic Nusselt numbers for four radius ratios of annulus, together with the analytic results discussed in the next section.

On Fig. 10, the results are plotted as a function

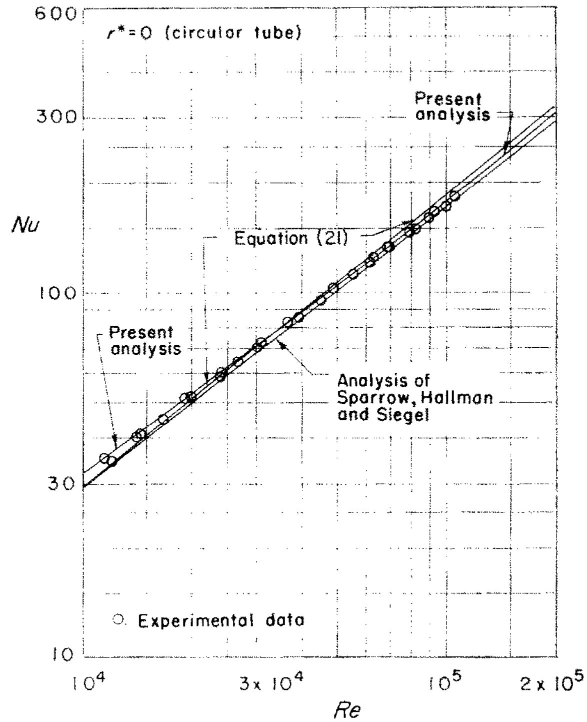

FIG. 5. Fully developed Nusselt numbers for flow in a circular tube, $Pr = 0.70$, constant heat rate.

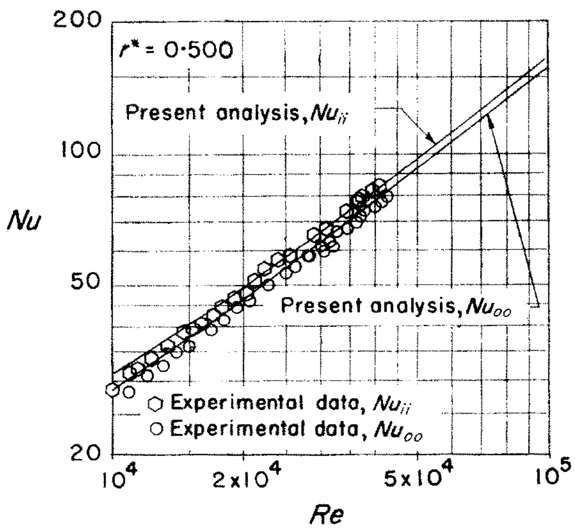

FIG. 6. Fully developed Nusselt numbers for $r^* = 0.500$, $Pr = 0.70$.

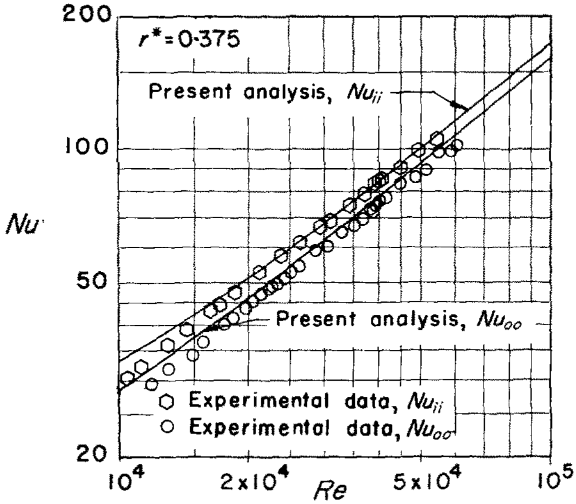

FIG. 7. Fully developed Nusselt numbers for $r^* = 0{\cdot}376$, $Pr = 0{\cdot}70$.

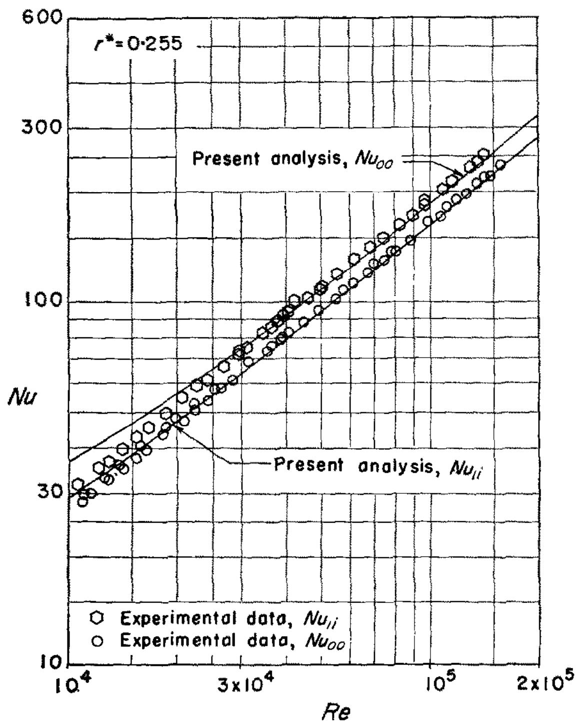

FIG. 8. Fully developed Nusselt numbers for $r^* = 0{\cdot}255$, $Pr = 0{\cdot}70$.

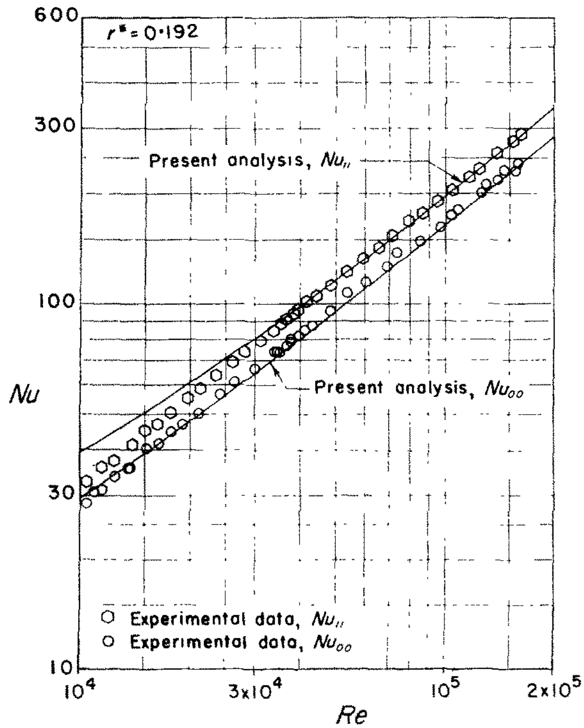

FIG. 9. Fully developed Nusselt numbers for $r^* = 0{\cdot}192$, $Pr = 0{\cdot}70$.

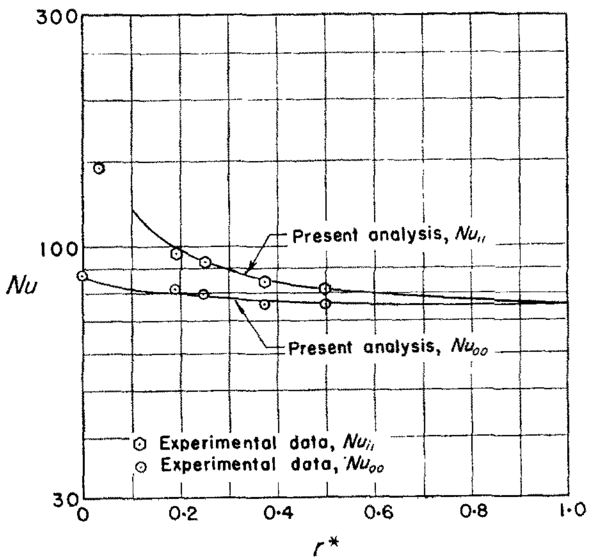

FIG. 10. Effect of radius ratio on fully developed Nusselt numbers, $Re = 40\,000$, $Pr = 0{\cdot}70$.

of radius ratio for one particular Reynolds number, 40 000, so that the effect of radius ratio can be clearly seen. Also included is the inner surface Nusselt number from the rather limited amount of data obtained at $r^* = 0{\cdot}029$.

ANALYSIS FOR FULLY DEVELOPED CONSTANT HEAT RATE

The large number of variables involved in the turbulent flow annulus heat transfer problem makes it rather impracticable to attempt to obtain a complete solution experimentally. Semi-empirical analytic solutions have been obtained for turbulent flow in a circular tube that are in very good agreement with experiment, and it would be very useful if the methods employed could be successfully extended to the annulus. In principle, the thermal entry length solutions can be obtained just as readily as the asymptotic solutions, but the computation problem becomes enormous, and only the asymptotic solutions are considered here.

Since what is believed to be good experimental data are now available for a fluid with $Pr = 0{\cdot}7$, the major purpose served by the analysis will be to extend the results to other Prandtl numbers. A fortunate feature of this problem is the fact that at very low Prandtl numbers, the problem approaches one of pure molecular conduction about which there is little uncertainty, while at very high Prandtl numbers, the heat-transfer resistance is concentrated so close to the wall surfaces that the geometry becomes of minor importance, and it is only necessary that the heat-transfer behavior of the sublayers be properly handled. The methods that have been successful for flow in a circular tube at high Prandtl numbers should be equally applicable here. Thus it is that the assumptions that must be made in the annulus heat-transfer analysis are most critical in the region near $Pr = 1{\cdot}00$, and it is, of course, in this region where we do have good experimental data to fall back upon. The analysis can be looked upon as an extrapolation of the experimental data, but a rather unique extrapolation in that the assumptions on which it is based become of decreasing consequence the farther the extrapolation is carried.

One of the major difficulties in the analysis of turbulent flow in a circular tube annulus is the determination of the ratio of the shear stresses on the two surfaces, and the related problem of determining the radius of maximum velocity, which is assumed to be the point of zero shear stress. If the radius of zero shear (maximum velocity) is designated as s, the relation between s and the surface stress ratio can be readily shown for fully developed flow to be,

$$\tau^* = \frac{\tau_o}{\tau_i} = \frac{(r_o^2 - s^2)}{(s^2 - r_i^2)} = \frac{(1 - \bar{s}^2)\, r^*}{(\bar{s}^2 - r^{*2})}, \quad \text{where } \bar{s} = s/r_o. \tag{22}$$

For laminar flow $\bar{s}$ is a unique function of r^* that can be easily evaluated, but there is no direct way to determine this function for turbulent flow, short of actually measuring it. Since a heat and momentum analogy method is to be used to calculate heat transfer, the shear stress distribution must be known. Note that this difficulty does not arise in the analysis of fully developed flow in a circular tube or between parallel planes (the two limiting cases of the annulus) because symmetry imposes a linear shear stress distribution for both laminar and turbulent flow.

A number of investigators have reported turbulent velocity profile measurements in circular tube annuli, and these provide probably the best source of data on shear–stress ratio. It is extremely difficult to measure shear stress directly, but the radius of maximum velocity can be scaled from velocity profile measurements, although because of the rather flat profile it is difficult to get high precision. On Fig. 11 the radius of maximum velocity, plotted in the form $s^* = (\bar{s} - r^*)/(1 - \bar{s})$ vs. r^*, is given from the authors' interpretation of profiles presented by Lorenz [6], Rothfus, Monrad, and Senecal [7], Knudsen and Katz [8], Owens [9], and Barrow [10]. Also shown on this plot is the laminar flow solution, and the result if the shear stresses on both surfaces were equal. The Reynolds numbers for these data vary from about 10 000 to over 700 000. Some of the investigators, notably Rothfus *et al.* and Barrow, conclude that the turbulent shear stress ratio is essentially the same as for laminar flow, but these results suggest a somewhat smaller ratio. There may well be a Reynolds number effect, in which case

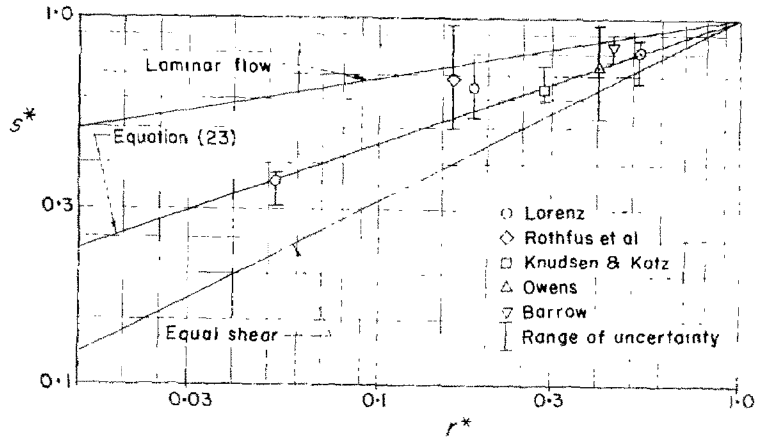

FIG. 11. Experimental data on the point of maximum velocity for turbulent flow in an annulus.

the fact that both the Rothfus and Barrow data are for moderately low Reynolds numbers may be significant. Of possibly greater significance is the fact that heat-transfer predictions based on the laminar shear stress ratio tend to yield Nusselt numbers on the inner surface that are considerably higher than measured, and it was only by using a lower curve that the authors were able to obtain predicted Nusselt numbers in good agreement with the heat-transfer measurements. The proposed curve,

$$s^* = (r^*)^{0\cdot 343} \tag{23}$$

was drawn so as to heavily weight the point at $r^* = 0{\cdot}052$ because this is believed to be the most accurate of all those plotted. Thus for the present analysis, equations (22) and (23) were used for the shear stress ratio, which then establishes the complete shear stress distribution.

Velocity and eddy diffusivity profile equations were developed by first breaking the flow area into four sections: (1) a sublayer near the inner surface; (2) a sublayer near the outer surface; (3) a fully turbulent region from the inner sublayer to the point of maximum velocity; (4) a fully turbulent region from the outer sublayer to the point of maximum velocity. The equations employed in these various regions will first be given, and then their origins will be discussed.

For both of the sublayers, the momentum eddy diffusivity was evaluated from,

$$\frac{\epsilon_M}{\nu} = m u_j^+ \eta_j^+ \, [1 - \exp(-m u_j^+ \eta_j^+)],$$

$$\text{where } m = 0{\cdot}0154. \tag{24}$$

The velocity profile in the sublayers was obtained by integration of the defining equation for total apparent shear stress, assuming the shear stress constant at the wall value, and using equation (24) for the diffusivity. This result cannot be put in a closed form equation. The sublayers were considered to extend to $\eta^+ = 42$, since it is at this point at which the sublayer velocity matches the fully turbulent region velocity.

The momentum eddy diffusivity equation for the region between the outer sublayer and the point of maximum velocity is,

$$\frac{\epsilon_M}{\nu} = \frac{(1 - \bar{s})\, r_o^+}{15} (1 - \eta_o^2)(1 + 2\eta_o^2) \, [1 + 0{\cdot}6(\eta_o - \eta_o^4)]. \tag{25}$$

The corresponding equation for the region from the point of maximum velocity to the inner surface sublayer is,

$$\frac{\epsilon_M}{\nu} = \frac{(1 - \bar{s})\, r_o^+}{15} (1 - \eta_i^2)(1 + 2\eta_i^2) \, [1 + 0{\cdot}6\sqrt{(r^*)}(\eta_i - \eta_i^4)] \left\{1 - \left[1 - \frac{\bar{s}\; r^*}{\sqrt{(r^*)}(1 - \bar{s})}\right]\eta_i\right\}. \tag{26}$$

The velocity equation used for the outer turbulent region is,

$$u_o^+ = 2{\cdot}5 \ln \eta_o^+ + 5{\cdot}5. \tag{27}$$

The corresponding velocity equation for the inner region is,

$$u_i^+ = \frac{1}{k_i} \ln \eta_i^+ + C_i \tag{28}$$

where k_i and C_i are variable coefficients chosen so that at all times (1) the velocity at the maximum velocity point matches the velocity equation from the outer surface, and (2) the velocity matches the sublayer velocity at $\eta_i^+ = 42$.

The sublayer diffusivity equation is essentially the equation proposed by Deissler [11] with a slightly modified independent variable. Deissler demonstrated that this equation works very well for heat-transfer calculations to high Prandtl number for circular tubes and there is no reason to believe that the sublayers on the annulus surfaces, should behave any differently than in a circular tube.

The turbulent region diffusivity equations, (25) and (26), are essentially modifications of the diffusivity expression proposed by Reichardt [12]. The momentum eddy diffusivity has been measured from a number of the velocity profiles presented in the above cited references, and two examples are shown in Figs. 12 and 13. The modifications to Reichardt's equation are purely empirical and were made to obtain a fit to the

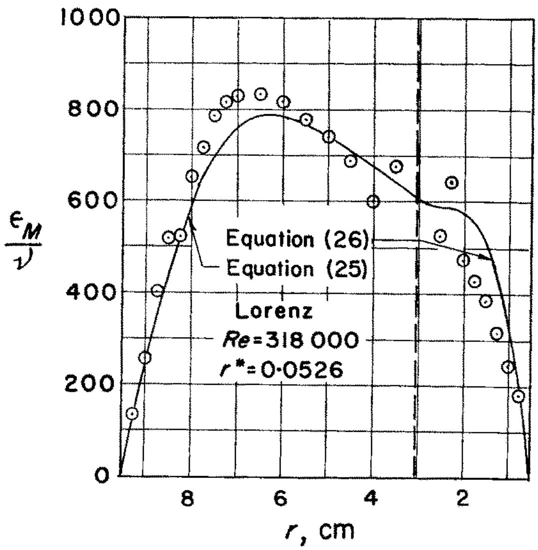

FIG. 12. Experimental data on momentum eddy diffusivity in an annulus.

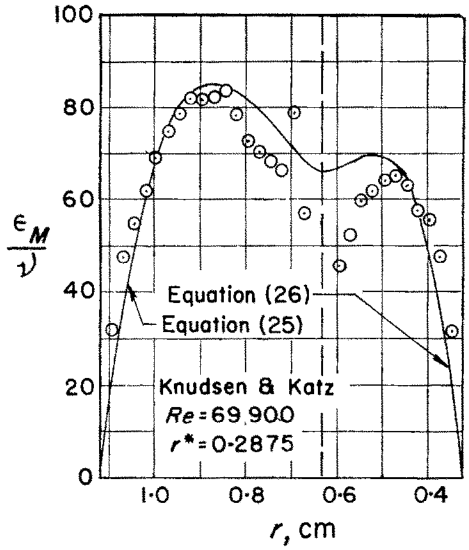

FIG. 13. Experimental data on momentum eddy diffusivity in an annulus.

measured diffusivities, as shown in the figures. As either of the surfaces are approached both equations approach $0{\cdot}4y^+$ which is the form predicted by mixing length theory and is consistent with all known measurements near a wall. Thus the modifications are primarily in the central region of the passage. For a symmetrically heated tube, accurate data on the diffusivity in the central region is not particularly important, but for the asymmetric type of heating considered here it is definitely necessary to have reasonably accurate data. The rather complex nature of the equations arises from the necessity of a pair of equations that will be adequate for all radius ratios, including the limiting cases of the circular tube and flow between parallel planes.

The two velocity profile equations, (27) and (28), are not derivable from the diffusivity equations, but do fit the available experimental data relatively well, as can be seen in Figs. 14 and 15. The inconsistency between the velocity and diffusivity equations is not important because nowhere in the computing procedure were the velocity equations differentiated. The velocity profiles could have been derived from the diffusivity equations and the shear stress distribution, but a considerable saving in computation time was effected by employing the

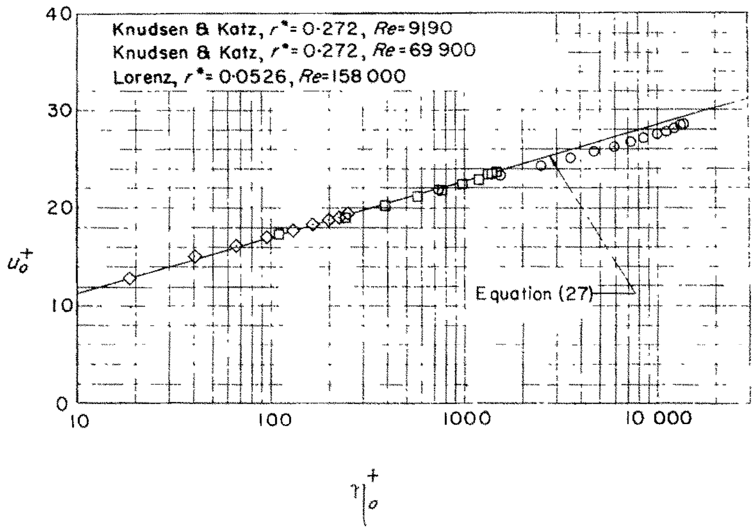

FIG. 14. Experimental velocity profiles in an annulus in the region between the point of maximum velocity and the outer surface sublayer.

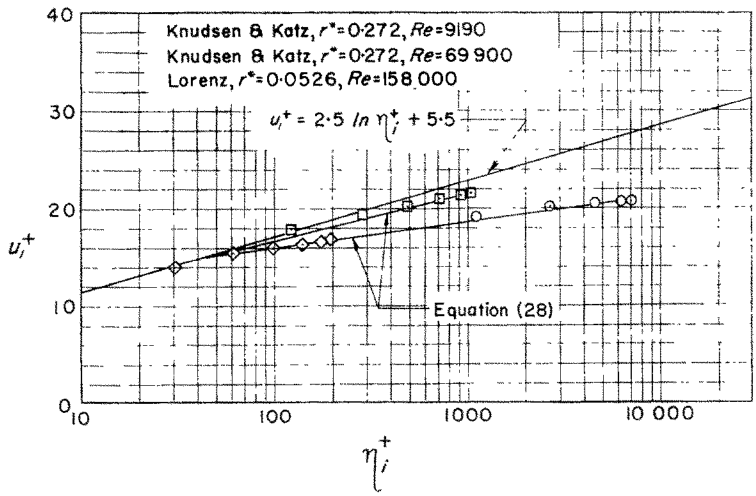

FIG. 15. Experimental velocity profiles in an annulus in the region between the inner surface sublayer and the point of maximum velocity.

simpler velocity equations. Equation (27) is recognized as the simple Nikuradse equation with the Reichardt middle law modification. Equation (28) is simply an empirical modification to fit the experimental data.

The essence of the heat and momentum analogy method of calculation lies in the assumption of a definite relationship between the thermal and momentum eddy diffusivities. The procedure used here was a modification of the procedure employed by Sleicher and Tribus [13]. The relationship calculated by Jenkins [14] was used, but the ratio of thermal to momentum eddy diffusivity was multiplied by a constant factor 1·20 so as to bring the calculated heat-transfer results for air in a circular tube into line with the experiments. However, in the sub-layers it was assumed that equation (24) could be used directly for thermal eddy diffusivity, i.e. that the diffusivities were always equal. The basis for this is that Deissler [11] employed equation (24) for a circular tube and obtained excellent correlation with experiments up to very high Prandtl numbers. At high Prandtl numbers the turbulent heat transfer behavior is very sensitive to the sublayer diffusivity, and rather insensitive to the diffusivity in the central region, whereas the reverse is true at low Prandtl number. It appears that for present purposes equation (24) can be looked upon as an expression for the thermal eddy diffusivity rather than the momentum eddy diffusivity.

The problem now is simply one of integrating equation (1) for the indicated boundary conditions employing the velocity and thermal eddy diffusivity data discussed above. Calculations were carried out only for the asymptotic solution, e.g. for points well downstream of the beginning of heating where a fully developed temperature profile is obtained. For constant heat rate per unit of tube length this can be accomplished by setting the derivative on the right-hand side of (1) equal to the mixed mean temperature gradient, which is a constant. The equation becomes an ordinary differential equation which can be readily solved numerically.

The calculations were carried out on a Burroughs 220 digital computer, and the results are presented in Table 1. The radius ratios considered include the limiting cases of the circular tube, $r^* = 0{\cdot}00$, and flow between parallel planes, $r^* = 1{\cdot}00$, as well as the annulus radius ratios 0·10, 0·20, 0·50, and 0·80. The Prandtl number was varied from 0·0 to 1000, and the Reynolds number from 10^4 to 10^6. Thus, a very extensive range of variables is covered with

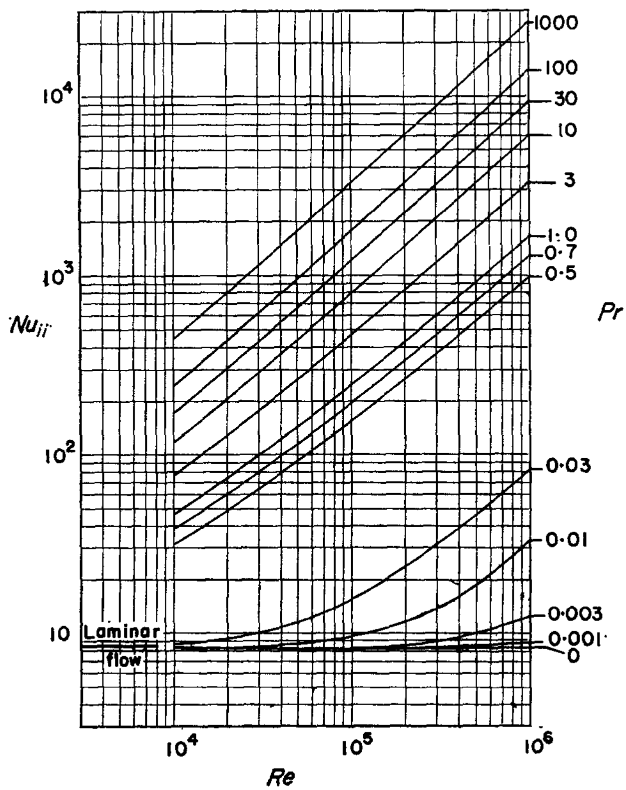

FIG. 16. Computed inner surface Nusselt numbers for fully developed velocity and temperature profiles for constant heat rate in an annulus with $r^* = 0{\cdot}20$.

Table 1

$r^* = 1{\cdot}00$, Parallel plates

Re → / Pr ↓	10^4		3×10^4		10^5		3×10^5		10^6	
Pr	Nu	θ^*	Nu	θ^*	Nu	θ^*	Nu	θ^*	Nu	θ^*
0	5·70	0·428	5·78	0·445	5·80	0·456	5·80	0·460	5·80	0·468
0·001	5·70	0·428	5·78	0·445	5·80	0·456	5·88	0·460	6·23	0·460
0·003	5·70	0·428	5·80	0·445	5·90	0·450	6·32	0·450	8·62	0·422
0·01	5·80	0·428	5·92	0·445	6·70	0·440	9·80	0·407	21·5	0·333
0·03	6·10	0·428	6·90	0·428	11·0	0·390	23·0	0·330	61·2	0·255
0·5	22·5	0·256	47·8	0·222	120	0·193	290	0·174	780	0·157
0·7	27·8	0·220	61·2	0·192	155	0·170	378	0·156	1030	0·142
1·0	35·0	0·182	76·8	0·162	197	0·148	486	0·138	1340	0·128
3	60·8	0·095	142	0·092	380	0·089	966	0·087	2700	0·084
10	101	0·045	241	0·045	680	0·045	1760	0·045	5080	0·046
30	147	0·021	367	0·022	1030	0·022	2720	0·023	8000	0·024
100	210	0·009	514	0·009	1520	0·010	4030	0·010	12 000	0·011
1000	390	0·002	997	0·002	2880	0·002	7650	0·002	23 000	0·002

$r^* = 0{\cdot}80$, Heating from outer tube

Re → / Pr ↓	10^4		3×10^4		10^5		3×10^5		10^6	
Pr	Nu_{oo}	θ_o^*	Nu_{oo}	θ_o^*	Nu_{oo}	θ_o^*	Nu_{oo}	θ_o^*	Nu_{oo}	θ_o^*
0	5·65	0·379	5·70	0·386	5·75	0·398	5·80	0·407	5·85	0·409
0·001	5·65	0·379	5·70	0·386	5·75	0·398	5·88	0·406	6·25	0·407
0·003	5·65	0·379	5·70	0·386	5·84	0·397	6·35	0·407	8·80	0·374
0·01	5·75	0·381	5·85	0·386	6·72	0·390	9·95	0·361	21·0	0·286
0·03	6·10	0·388	6·90	0·380	11·1	0·339	23·2	0·290	62·0	0·216
0·5	22·4	0·225	48·0	0·191	121	0·169	292	0·153	790	0·136
0·7	28·0	0·192	61·0	0·166	156	0·150	378	0·136	1020	0·122
1·0	34·8	0·159	76·5	0·141	197	0·129	483	0·120	1330	0·111
3	61·3	0·083	142	0·079	382	0·078	960	0·076	2730	0·073
10	100	0·039	243	0·039	670	0·039	1740	0·040	5050	0·040
30	146	0·019	365	0·019	1040	0·020	2720	0·021	8000	0·022
100	209	0·008	533	0·008	1500	0·009	4000	0·009	12 000	0·101
1000	385	0·002	1000	0·002	2870	0·002	7720	0·002	23 000	0·002

$r^* = 0{\cdot}80$, Heating from core tube

Re → / Pr ↓	10^4		3×10^4		10^5		3×10^5		10^6	
Pr	Nu_{ii}	θ_i^*	Nu_{ii}	θ_i^*	Nu_{ii}	θ_i^*	Nu_{ii}	θ_i^*	Nu_{ii}	θ_i^*
0	5·87	0·489	5·90	0·505	5·92	0·515	5·95	0·525	5·97	0·528
0·001	5·87	0·489	5·90	0·505	5·92	0·515	6·00	0·518	6·33	0·516
0·003	5·87	0·489	5·90	0·505	6·03	0·485	6·40	0·504	8·80	0·468
0·01	5·95	0·485	6·07	0·506	6·80	0·493	10·0	0·452	21·7	0·382
0·03	6·20	0·478	7·05	0·485	11·4	0·445	23·0	0·357	61·0	0·276
0·5	22·9	0·268	49·5	0·250	123	0·214	296	0·193	800	0·174
0·7	28·5	0·244	62·3	0·212	157	0·186	384	0·172	1050	0·160
1·0	35·5	0·200	78·3	0·181	202	0·166	492	0·154	1350	0·140
3	63·0	0·108	145	0·102	386	0·097	973	0·096	2750	0·093
10	102	0·051	248	0·051	693	0·052	1790	0·051	5150	0·051
30	147	0·027	370	0·027	1050	0·028	2750	0·029	8100	0·030
100	215	0·010	540	0·010	1540	0·010	4050	0·011	12 000	0·012
1000	393	0·002	1000	0·002	2890	0·002	7700	0·002	23 000	0·002

$r^* = 0{\cdot}50$, Heating from outer tube

Re → / Pr ↓	10^4		3×10^4		10^5		3×10^5		10^6	
Pr	Nu_{oo}	θ_o^*	Nu_{oo}	θ_o^*	Nu_{oo}	θ_o^*	Nu_{oo}	θ_o^*	Nu_{oo}	θ_o^*
0	5·66	0·281	5·78	0·294	5·80	0·296	5·83	0·302	5·95	0·310
0·01	5·66	0·281	5·78	0·294	5·80	0·296	5·92	0·302	6·40	0·304
0·003	5·66	0·281	5·78	0·294	5·85	0·294	6·45	0·301	9·00	0·278
0·01	5·73	0·281	5·88	0·289	6·80	0·289	10·3	0·264	22·6	0·217
0·03	6·03	0·279	7·05	0·284	11·6	0·258	24·4	0·214	64·0	0·163
0·5	22·6	0·162	49·8	0·142	125	0·123	298	0·111	795	0·098
0·7	28·3	0·137	62·0	0·119	158	0·107	380	0·097	1040	0·090
1·0	34·8	0·111	78·0	0·101	200	0·092	490	0·085	1340	0·078
3	60·5	0·059	144	0·058	384	0·055	960	0·054	2730	0·052
10	100	0·028	246	0·028	680	0·028	1750	0·028	5030	0·028
30	143	0·013	365	0·013	1030	0·014	2700	0·014	8000	0·015
100	207	0·006	530	0·006	1500	0·006	4000	0·006	12 000	0·006
1000	387	0·001	990	0·001	2830	0·001	7600	0·001	23 000	0·001

Table 1—*continued*

$r^* = 0{\cdot}50$, Heating from core tube

Re	10^4		3×10^4		10^5		3×10^5		10^6	
Pr	Nu_{ii}	θ_i^*	Nu_{ii}	θ_i^*	Nu_{ii}	θ_i^*	Nu_{ii}	θ_i^*	Nu_{ii}	θ_i^*
0	6·28	0 620	6 30	0·632	6 30	0 651	6·30	0·659	6 30	0 654
0·01	6 28	0 620	6·30	0 632	6·30	0·651	6·40	0·659	6·75	0·644
0 003	6 28	0·620	6·30	0·632	6·40	0·656	6·85	0·637	9·40	0·585
0 01	6·37	0·622	6·45	0 636	7·30	0 623	10·8	0·540	23·2	0·427
0·03	6·75	0 627	7·53	0·598	12·0	0·533	24 8	0 430	65·5	0·333
0·5	24·6	0·343	52 0	0·292	130	0·253	310	0·229	835	0·208
0 7	30 9	0·300	66·0	0·258	166	0·225	400	0·206	1080	0·185
1·0	38·2	0·247	83·5	0·218	212	0·208	520	0·183	1420	0·170
3	66·8	0·219	152	0·121	402	0·115	1010	0·114	2870	0·111
10	106	0·059	260	0·059	715	0·059	1850	0·059	5400	0 061
30	153	0 028	386	0·027	1080	0·028	2850	0·031	8400	0·032
100	220	0·006	558	0·006	1600	0·006	4250	0·007	12 600	0·007
1000	408	0 002	1040	0·002	3000	0 002	8000	0·002	24 000	0·002

$r^* = 0{\cdot}20$, Heating from outer tube

Re	10^4		3×10^4		10^5		3×10^5		10^6	
Pr	Nu_{oo}	θ_o^*	Nu_{oo}	θ_o^*	Nu_{oo}	θ_o^*	Nu_{oo}	θ_o^*	Nu_{oo}	θ_o^*
0	5·83	0 140	5 92	0·145	6·10	0·151	6·16	0·152	6·35	0·157
0·001	5 83	0·140	5·92	0·144	6 10	0·151	6·30	0·154	6·92	0·153
0 003	5·83	0·140	6·00	0·146	6·22	0·150	6·90	0·150	10·2	0·136
0·01	5·95	0 140	6·20	0 146	7·40	0·144	11·4	0·131	24·6	0·102
0·03	6 22	0·140	7·55	0·140	12·7	0·125	26·3	0 098	80·0	0·074
0 5	22·5	0·071	51·5	0·064	130	0·055	310	0·049	823	0·044
0·7	29 4	0·063	64·3	0·055	165	0 049	397	0·044	1070	0 040
1·0	35·5	0 051	80 0	0·046	206	0·042	504	0·039	1390	0·035
3	60 0	0·026	145	0 026	390	0·024	980	0·024	2760	0·023
10	98·0	0·013	243	0 013	680	0·012	1750	0 012	4980	0·012
30	142	0·006	360	0·006	1030	0·006	2700	0·006	7850	0·006
100	205	0·003	520	0·003	1500	0·003	4000	0·003	12 000	0·003
1000	380	0·001	980	0 001	2830	0·001	7500	0·001	22 500	0·001

$r^* = 0{\cdot}20$, Heating from core tube

Re	10^4		3×10^4		10^5		3×10^5		10^6	
Pr	Nu_{ii}	θ_i^*	Nu_{ii}	θ_i^*	Nu_{ii}	θ_i^*	Nu_{ii}	θ_i^*	Nu_{ii}	θ_i^*
0	8·40	1 009	8·30	1·028	8·30	1·020	8·30	1·038	8·30	1·020
0 001	8 40	1·009	8 40	1·040	8 30	1·020	8·40	1·014	8·90	0·976
0 003	8·40	1·009	8·40	1·027	8·50	1·025	9·05	0·980	12·5	0·834
0·01	8·50	1·000	8·60	1·018	9 70	0·944	14·0	0·796	33·6	0·748
0·03	9·00	1·012	10·1	0·943	15·8	0·771	31·7	0·600	81·0	0·374
0·5	31·2	0·520	64·0	0·398	157	0·333	370	0·295	980	0·262
0·7	38·6	0 412	79·8	0·338	196	0 286	473	0·260	1270	0·235
1·0	46 8	0·339	99·0	0·284	247	0·248	600	0·229	1640	0·209
3	77·4	0 172	175	0·151	465	0·143	1150	0·137	3250	0·135
10	120	0 077	290	0·074	800	0·072	2050	0·073	6000	0·077
30	172	0·036	428	0·034	1210	0·035	3150	0·036	9300	0·038
100	243	0·014	617	0·014	1760	0·015	4630	0·016	13 800	0·016
1000	448	0 004	140	0 002	3280	0·002	8800	0·004	26 000	0·003

$r^* = 0{\cdot}10$, Heating from outer tube

Re	10^4		3×10^4		10^5		3×10^5		10^6	
Pr	Nu_{oo}	θ_o^*	Nu_{oo}	θ_o^*	Nu_{oo}	θ_o^*	Nu_{oo}	θ_o^*	Nu_{oo}	θ_o^*
0	6·00	0·077	6·12	0·079	6·32	0·081	6·50	0·084	6·68	0·085
0 001	6·00	0·077	6·12	0·079	6·40	0·082	6·60	0·082	7·20	0·082
0·003	6·00	0 077	6·24	0·081	6·55	0·083	7·34	0·082	10·8	0 071
0·01	6·13	0·076	6·50	0·081	7 80	0·077	12·1	0·067	26·4	0·052
0·03	6·45	0·076	7 95	0 075	13·7	0·065	28·2	0 051	71·8	0·036
0 5	24·8	0 039	53 4	0·032	134	0·028	320	0·025	860	0·022
0·7	29·8	0·032	66·0	0·028	167	0·024	409	0·022	1100	0·020
1·0	36·5	0·026	81·8	0·023	212	0 021	520	0·019	1430	0·017
3	61·5	0·013	147	0 013	395	0·012	1000	0·012	2830	0·011
10	99·2	0·006	246	0·006	685	0·006	1780	0·006	5200	0·006
30	143	0·003	360	0·003	1030	0·003	2720	0·003	8030	0·003
100	205	0·002	525	0·002	1500	0·002	4030	0·002	12 100	0·002
1000	378	—	980	—	2850	—	7600	—	23 000	—

Table 1—*continued*

$r^* = 0{\cdot}10$, Heating from core tube

Pr \ Re	10^4		3×10^4		10^5		3×10^5		10^6	
Pr	Nu_{ii}	θ_i^*	Nu_{ii}	θ_i^*	Nu_{ii}	θ_i^*	Nu_{ii}	θ_i^*	Nu_{ii}	θ_i^*
0	11·5	1·475	11·5	1·502	11·5	1·500	11·5	1·460	11·6	1·477
0·001	11·5	1·475	11·5	1·502	11·5	1·480	11·7	1·462	12·3	1·410
0·003	11·5	1·475	11·5	1·475	11·7	1·473	12·6	1·391	17·0	1·124
0·01	11·8	1·482	11·8	1·442	13·5	1·323	19·4	1·090	39·0	0·760
0·03	12·5	1·472	14·1	1·330	21·8	1·027	42·0	0·760	103	0·526
0·5	40·8	0·632	81·0	0·486	191	0·394	443	0·339	1160	0·294
0·7	48·5	0·512	98·0	0·407	235	0·338	550	0·292	1510	0·269
1·0	58·5	0·412	120	0·338	292	0·286	700	0·256	1910	0·232
3	93·5	0·202	206	0·175	535	0·162	1300	0·152	3720	0·148
10	140	0·089	328	0·081	890	0·078	2300	0·078	6700	0·077
30	195	0·041	478	0·039	1320	0·038	3470	0·038	10 300	0·040
100	272	0·017	673	0·015	1910	0·015	5030	0·016	15 200	0·018
1000	486	0·004	1240	0·003	3600	0·003	9600	0·004	28 700	0·004

$r^* = 0$, Circular tube

Pr \ Re	10^4	3×10^4	10^5	3×10^5	10^6
Pr	Nu	Nu	Nu	Nu	Nu
0	6·30	6·64	6·84	6·95	7·06
0·001	6·30	6·64	6·84	7·08	8·12
0·003	6·30	6·64	7·10	8·14	12·8
0·01	6·43	7·00	8·90	14·2	30·5
0·03	6·90	9·10	15·9	32·4	80·5
0·5	26·3	57·3	142	340	895
0·7	31·7	70·7	178	430	1150
1·0	37·8	86·0	222	543	1470
3	61·5	149	404	1030	2900
10	99·8	248	690	1810	5220
30	141	362	1030	2750	8060
100	205	522	1510	4030	12 000
1000	380	975	2830	7600	22 600

a single computing procedure. The results consist of the Nusselt number for one side only heated, and the influence coefficients. Employing equations (15) and (16) the Nusselt number on either side of an annular passage may be computed for any heat flux ratio, positive or negative.

The computed Nusselt numbers for one radius ratio only, $r^* = 0{\cdot}20$, are plotted on Figs. 16 and 17. The data for the other radius ratios in Table 1 would appear similar if plotted. A cross-plot at a Reynolds number of 40 000 is shown on Fig. 10. A comparison of the analysis with the experiments at $Pr = 0{\cdot}7$ is given in Figs. 5–10, and the comparison is excellent, except at Reynolds numbers below 30 000 where, especially for the inner surface of the annulus, the analysis tends to over-predict the Nusselt number by up to 10 per cent. The reason for this discrepancy is not at present understood.

One word of precaution in using this data should be added. It can be shown for laminar flow that longitudinal conduction begins to be a significant factor if the product, $Re \cdot Pr$, is less than 100. Since longitudinal conduction has been neglected in this analysis, the Nusselt numbers in Table 1 for which $Re \cdot Pr < 100$ are undoubtedly over-predictions. Longitudinal conduction may be the difficulty in the low Reynolds number experiments discussed above because the longitudinal turbulent eddy conductivity has been neglected.

EXPERIMENTAL RESULTS FOR ASYMMETRIC HEATING

The experimental apparatus was designed so that it could be used for asymmetric heating as well as for heating from one side of the annulus only. Asymmetric heating tests were run as a check on the fundamental solution theory, and also as a further check on the accuracy of the fundamental solutions. On Figs. 18 and 19 some examples of the results of the asymmetric heating tests are shown, together with the predicted performance. The predicted performance is based on the fundamental solutions presented in Figs. 1, 2, 3, and 4 so that the effects of thermal entry length are included.

The agreement between theory and experiment appears to be excellent. A reasonably wide range of heat flux ratio was employed, 0·689–15·5, with equally good results in all cases. Note that heat flux ratio can have a large influence on Nusselt number, and that the outer tube Nusselt number can be either above or below the inner tube Nusselt number depending upon heat flux ratio.

SUMMARY AND CONCLUSIONS

In this paper the Fundamental Solutions of the Second Kind are partially developed for turbulent flow in a circular tube annulus. The accomplishments of the paper may be summarized as follows.

1. The asymptotic Fundamental Solutions of the Second Kind for turbulent flow are developed analytically for a wide range of radius ratio, Reynolds number, and Prandtl number. These results have been checked experimentally at $Pr = 0{\cdot}7$, and there is reason to believe that they are equally valid at very high and very low

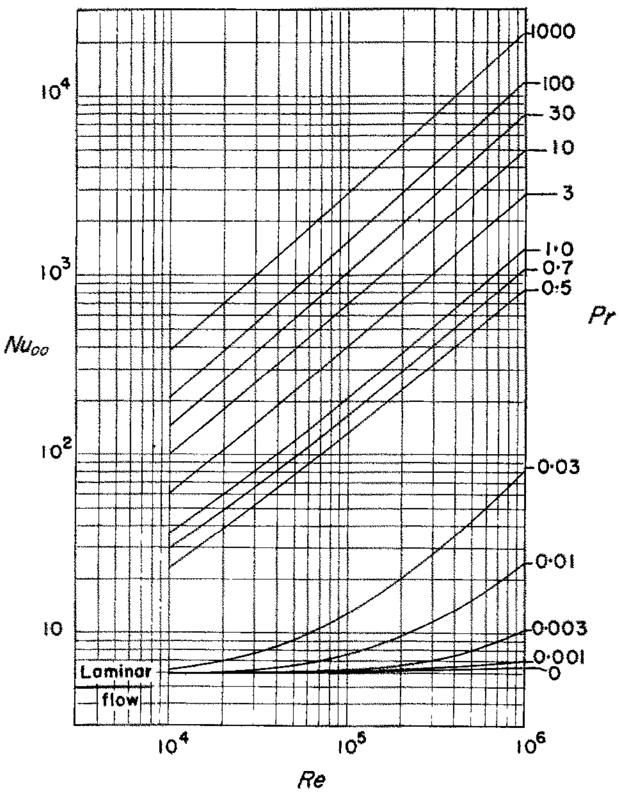

FIG. 17. Computed outer surface Nusselt numbers for fully developed velocity and temperature profiles for constant heat rate in an annulus with $r^* = 0{\cdot}20$.

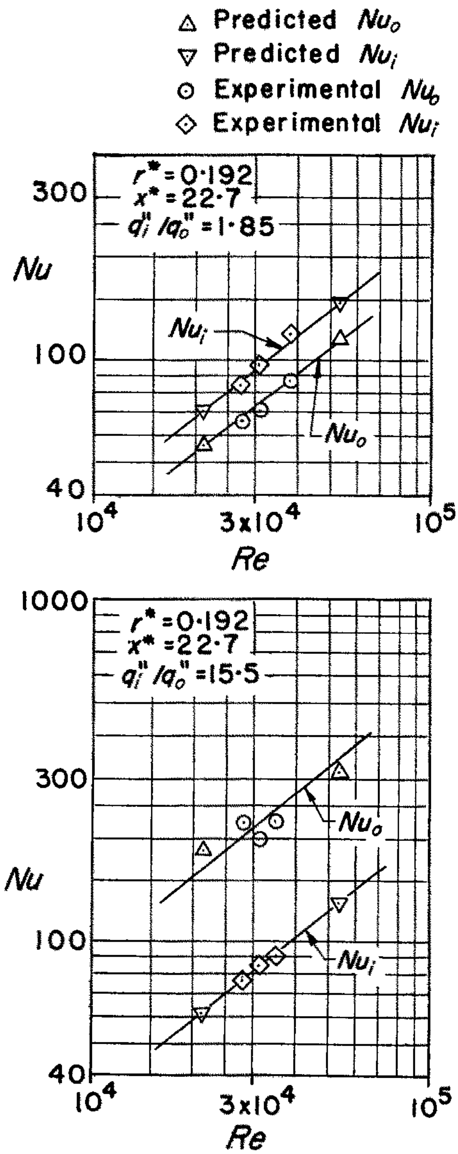

FIG. 18. Comparison of analysis and experiment for an asymmetrically heated annulus.

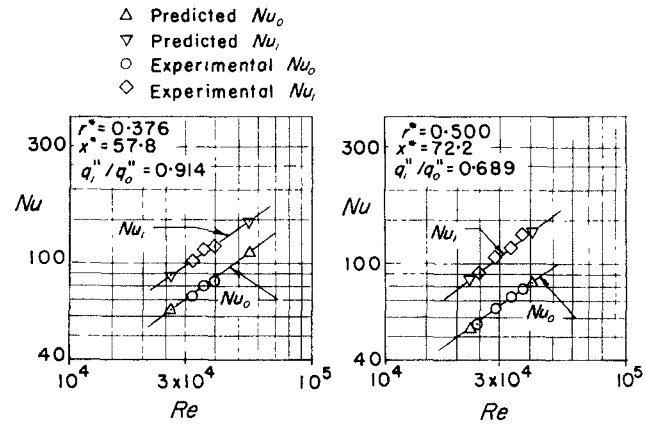

FIG. 19. Comparison of analysis and experiment for an asymmetrically heated annulus.

Prandtl numbers. The cases of the circular tube and flow between parallel planes have been included as the limiting cases of the annulus geometry, and as far as the authors are aware, this is the first time that a single consistent analysis for the entire Prandtl number spectrum has been attempted even for these limiting cases.

2. The complete Fundamental Solution of the Second Kind is developed from experimental data for a fluid with $Pr = 0{\cdot}7$. With this solution the thermal entry length problem may be handled, and superposition may be used to solve any heat flux distribution in the direction of flow.

3. The method of superposition of fundamental solutions to solve for any arbitrary heat flux ratio on the two surfaces of an annulus is demonstrated and verified experimentally.

ACKNOWLEDGEMENTS

The work on which this paper is based was made possible by a grant (NSG-52-60) from The National Aeronautical and Space Administration. The authors express their appreciation for this assistance.

The assistance of Mr. Frank Incropera in obtaining the experimental data at $r^* = 0{\cdot}029$ is gratefully acknowledged. The experimental apparatus was largely designed and built by Mr. R. E. Lundberg and Mr. H. S. Heaton, and their contribution to the success of the program was very substantial indeed.

REFERENCES

1. W. C. REYNOLDS, R. E. LUNDBERG and P. A. MCCUEN, Heat transfer in annular passages—General formulation of the problem for arbitrarily prescribed wall temperatures or heat fluxes, *Int. J. Heat Mass Transfer*, **6**, 483 (1963).
2. R. E. LUNDBERG, P. A. MCCUEN and W. C. REYNOLDS, Heat transfer in annular passages—Hydrodynamically developed laminar flow with arbitrarily prescribed wall temperatures or heat fluxes, *Int. J. Heat Mass Transfer*, **6**, 495 (1963).
3. E. Y. LEUNG, W. M. KAYS and W. C. REYNOLDS, Heat transfer with turbulent flow in concentric and eccentric annuli with constant and variable heat flux. Report No. AHT-4, Thermosciences Division, Department of Mechanical Engineering, Stanford University, Stanford, California (available through Stanford University Library).
4. L. V. HUMBLE, W. H. LOWDERMILK and L. G. DESMON, Measurement of average heat transfer and friction coefficients for subsonic flow of air in smooth tubes at high surface and fluid temperatures. *NACA* Report 1020 (1951).
5. E. M. SPARROW, T. M. HALLMAN and R. SIEGEL, Turbulent heat transfer in the thermal entrance region of a pipe with uniform heat flux, *Appl. Sci. Res.* A7, 37–52 (1958).
6. F. R. LORENZ, On turbulent flow through annular passages. Communications, Institute of Fluid Mechanics, Karlsruhe (1932).
7. R. R. ROTHFUS, C. C. MONRAD and V. E. SENECAL, Velocity distribution and fluid friction in smooth concentric annuli, *Industr. Engng Chem.* **42**, 2511–2520 (1950).
8. J. G. KNUDSEN and D. L. KATZ, Velocity profiles in annuli. Proceedings of the First Midwestern Conference on Fluid Mechanics (1950).
9. W. M. OWEN, Experimental study of water flow in annular pipes, *Proc. ASCE*, **77**, Separate No. 88 (1951).
10. H. BARROW, Fluid flow and heat transfer in an annulus with a heated core tube. General Discussion on Heat Transfer, 1113–1122, London (1951).
11. R. G. DEISSLER, Analysis of turbulent heat transfer, mass transfer, and fluid friction in smooth tubes at high Prandtl and Schmidt numbers. *NACA* Report 1210 (1955).

12. H. REICHARDT, Complete representation of turbulent velocity in a smooth pipe, *Z. Angew. Math. Mech.* **31**, 208 (1951).
13. C. A. SLEICHER and M. TRIBUS, Heat transfer in a pipe with turbulent flow and arbitrary wall temperature distribution. Heat Transfer and Fluid Mechanics Institute, 59–78, Stanford University (1956).
14. R. JENKINS, Variation of the eddy conductivity with Prandtl modulus and its use in prediction of turbulent heat transfer coefficients. Heat Transfer and Fluid Mechanics Institute, 147, Stanford University (1951).

Résumé—On considère le problème de la transmission de chaleur dans le cas d'un écoulement turbulent dans une conduite annulaire, le profil des vitesses et le flux de chaleur par unité de longueur étant constants. Les solutions expérimentales obtenues pour des longueurs d'établissement du régime thermique d'un fluide de $Pr = 0{,}7$ sont présentées. Les solutions asymptotiques (profils de température et de vitesse en régime établi) sont données pour un grand domaine de rapports de rayons, de nombres de Reynolds et de nombres de Prandtl. Les solutions sont basées sur des profils de vitesse et de diffusivité turbulente empiriques, et la validité des solutions est expérimentalement démontrée pour $Pr = 0{,}7$. Une méthode de superposition est proposée pour résoudre le cas d'un chauffage asymétrique des deux parois de l'anneau, les données expérimentales obtenues dans ce cas sont en bon accord avec les résultats du calcul. Cet article est le 3ème d'une série (1, 2) qui termine quatre années d'études sur la transmission de chaleur dans les passages annulaires.

Zusammenfassung—Es wird das Problem des Wärmeüberganges in turbulenter Strömung in einem konzentrischen Ringraum bei ausgebildetem Geschwindigkeitsprofil und konstanter Wärmezufuhr pro Längeneinheit behandelt. Versuchsergebnisse sind für die thermische Einlauflänge für eine Flüssigkeit mit $Pr = 0{,}7$ angegeben. Asymptotische Lösungen (ausgebildetes Geschwindigkeits- und Temperaturprofil) wurden für einen grossen Bereich von Radiusverhältnissen, Reynoldszahlen und Prandtlzahlen ausgearbeitet. Die Lösungen beruhen auf empirischen Geschwindigkeitsprofilen und Profilen für turbulenten Austausch, wobei ihre Gültigkeit experimentell für $Pr = 0{,}7$ gezeigt wird. Eine Überlagerungsmethode dient zur Lösung des Problems der asymetrischen Beheizung von den beiden Oberflächen eines Ringraumes her. Versuchsergebnisse für asymmetrische Beheizung zeigen ausgezeichnete Übereinstimmung mit der Analyse. Diese Arbeit ist die dritte einer Reihe (1, 2) die über eine vierjährige Forschungstätigkeit über Wärmeübergang in Ringräumen berichtet.

Аннотация—Рассмотрена задача о теплообмене при турбулентном течении в концентрическом кольцевом канале с полностью развитым профилем скорости и постоянной скоростью обогрева на единицу длины. Экспериментальным путем получены решения для входного участка стабилизации нагрева при $Pr = 0{,}7$ для газа. Получены асимптотические решения (полностью развитые профили скорости и температуры) для широкого диапазона изменения отношения радиусов канала, критериев Рейнольдса и Прандтля. Решения основаны на полученных экспериментально профилях скорости и турбулентной диффузии. Справедливость решений подтверждена опытными данными при $Pr = 0{,}7$. Для решения задачи об асимметричном нагреве поверхностей канала использован метод суперпозиции. Приведенные экспериментальные данные по асимметричному нагреву хорошо согласуются с теоретическими. Эта статья является третьей в серии (1, 2) и завершает четырехлетнее исследование теплообмена в кольцевых каналах.